SHARPENING-DEMOSAICKING METHOD FOR REMOVAL OF IMAGE BLURS CAUSED BY AN OPTICAL LOW-PASS FILTER

Takashi Komatsu Takahiro Saito
Dept. of EEI Engineering, High-Tech Research Center, Kanagawa University, Yokohama, Japan
e-mail: { komatt01, saitot01}@kanagawa-u.ac.jp

ABSTRACT

The optical low-pass filter used for a digital camera is formed by combining two types of doubly refractive crystal device. Since the filter cannot sharply cut off high frequency components and it reduces frequency components under the Nyquist frequency, images projected on the imaging surface are blurred. This paper presents a demosaicking method that simultaneously removes image blurs caused by the optical low-pass filter. Our sharpening-demosaicking method employs the Landweber-type iterative algorithm. Since the Bayer's RGB color filter array is not necessarily proper for our method, we study another better color filter array, the WRB filter array where the W-filtering means that all the visible light passes through it. Our sharpening-demosaicking approach is formulated as the least square problem, but it has multiple solutions. To avoid the ambiguity, we introduce the frequency-band limitation corresponding to the mosaicking pattern of color filters, into the iterative algorithm.

1. INTRODUCTION

To suppress aliasing artifacts caused by the mosaicking on the imaging surface, a digital camera uses an optical low-pass filter that cuts off frequency components higher than the Nyquist frequency. A doubly refractive crystal device is widely used as an optical low-pass filter. This filter cannot sharply cut off high frequency components and hence images projected on the imaging surface are blurred.

This paper presents a new demosaicking method that simultaneously removes image blurs caused by the optical-low pass filter. Most of the existing demosaicking methods [1~3] such as the adaptive color plan interpolation method (ACPI) [3] try to interpolate intensity of non-observed color pixels, but do not try to remove image blurs caused by the optical low-pass filter. To remove the image blurs, the observed blurred color pixels as well as the non-observed color pixels should be sharpened in the middle of the demosaicking. Recently Malgouyres and Guichard have studied the deblurring-oversampling problem for monochrome images from a mathematical point of view [4], whereas in this paper we study the sharpening-demosaicking problem for mosaicked color images from a practical point of view.

The imaging process is formulated by

$$g = A \bullet f \tag{1}$$

where f is an original non-mosaicked image, A represents the imaging process consisting of the optical low-pass filtering, the color-component separation and the sub-sampling, and g is a mosaicked image. Since the imaging process is irreversible, our sharpening-demosaicking approach is formulated as the least square problem whose solution is given by the pseudo inverse operator A^+ of the imaging process A as follows:

$$f = A^+ \bullet g \tag{2}$$

To solve this problem, we employ the Landweber-type iterative restoration algorithm [5, 6]. As Trussel and Hartwing have recently pointed out [7], in the case of the Bayer's primary color filter array, the demosaicking problem of equation (2) can be solved by the non-iterative explicit approach; but their non-iterative approach does not take into account removal of the image blurs caused by the optical low-pass filter, and it is possible but highly complicated to extend the non-iterative approach to the sharpening-demosaicking problem using the WRB color filter array that will be described in the following sections. On the other hand, it is easy to extend the Landweber-type iterative algorithm. However, in this case the problem has multiple solutions. To avoid the ambiguity, we introduce the frequency-band limitation corresponding to the mosaicking pattern of color filters, into the iterative algorithm.

For our sharpening-demosaicking method, the Bayer's RGB color filter array is not necessarily proper. If the Bayer's RGB filter array is employed, the restored red and blue images will not be sharpened to the same degree as the restored green image. For our sharpening-demosaicking method, the WRB filter array is preferable to the RGB filter array, where the W filtering means that all the visible light passes through it. We experimentally show that our sharpening-demosaicking method separates each W intensity into three values of the RGB primary colors successfully and reconstructs a sharpness-improved RGB color image.

2. OPTICAL LOW-PASS FILTER

The optical low-pass filter is formed by combining two types of doubly refractive crystal device; the one separates its incident light into two traveling directions horizontally spaced each other by one pixel, and the other does vertically spaced by one pixel. On the imaging surface the optical low-pass filter projects a blurred continuous image, which is equivalent to summing up four shifted continuous images: the original continuous image and the horizontally, vertically and diagonally shifted images. Each pixel intensity is given by the spatial integration of intensity within the four corresponding image portions each of which is defined in each of the four shifted continuous images. Moreover, assuming that each pixel has a 100% aperture, then each pixel intensity will be given by the spatial integration of intensity within the image portion

0-7803-8554-3/04/$20.00 ©2004 IEEE.

of the size of vertically and horizontally twice the pixel interval.

The frequency response of the imaging process is formulated as follows. As for a one-dimensional signal $I[x]$, the image-duplication caused by the doubly refractive crystal device is formulated by

$$O[x] = I[x] + I[x-1] \tag{3}$$

where $I[x]$ corresponds to the incident light and $O[x]$ corresponds to the output. The transfer function H_D of the image-duplication is given by

$$H_D(e^{j\omega}) = 1 + e^{-j\omega D} \tag{4}$$

where D is the pixel interval. The optical low-pass filter does not sharply cut off high frequency components, and it reduces frequency components lower than the Nyquist frequency. Hence, observed color pixels suffer from image blurs. Moreover, taking into account the hold process of the 100 % aperture in the sampling, we get the total transfer function H_T:

$$H_T(\omega) = (1 + e^{-j\omega D}) \cdot \{ \sin(\omega D/2) / (\omega D/2) \} \tag{5}$$

3. SHARPENING-DEMOSAICKING METHOD FOR THE BAYER'S RGB COLOR FILTER ARRAY

3.1. Sharpening-demosaicking method

There exist cross-correlations among RGB color components of natural images. However, it is unpromising to define the generic cross-correlations among the three primary colors, because the cross-correlations heavily depend on image contents. Digital cameras should be capable of taking high-quality images for all kinds of scene. Therefore, this paper does not utilize the cross-correlations for the sharpening-demosaicking approach. We apply the Landweber-type iterative sharpening-demosaicking algorithm to each primary color component separately.

The Landweber-type algorithm solves the sharpening-demosaicking problem by starting with an initial demosaicked green image $G_{rec}^{(0)}$ and then updating its demosaicked green image $G_{rec}^{(n)}$ iteratively by the recurrence formula:

$$G_{rec}^{(n+1)} = G_{rec}^{(n)} + \varepsilon \cdot A^* \bullet (G_{obs} - A \bullet G_{rec}^{(n)}) \tag{6}$$

where G_{obs} is the observed mosaicked green image, the operator A means the imaging process including the spatial integration of intensity within the image portion of the size of vertically and horizontally twice the pixel interval as described in section 2, and the operator A^* is the adjoint operator of the operator A. The update coefficient ε is a constant to control the convergence speed. $G_{rec}^{(n)}$ converges to an attracting fixed point as long as we set ε to a proper value. Unfortunately, there exit a number of convergent solutions. To prevent the ambiguity of the solution, we introduce the frequency-band limitation into the recursion formula, as follows:

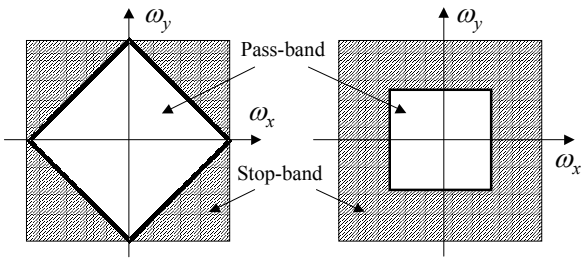

(a) Mosaicked green pixels (b) Mosaicked red and blue pixels

Figure 1: Fundamental frequency pass-band.

$$G_{rec}^{(n+1)} = L_g \left[G_{rec}^{(n)} + \varepsilon \cdot A^* \bullet (G_{obs} - A \bullet G_{rec}^{(n)}) \right] \tag{7}$$

, L_g : frequency-band limitation for the green plane

where the operator L_g limits the frequency components of the updated image $G_{rec}^{(n)}$ within the fundamental frequency pass-band corresponding to the sub-sampling pattern of the mosaicked green pixels and here we form it as the band limitation in the DFT domain. Figure 1(a) illustrates this frequency-band limitation.

In the same way, the red image and the blue image are interpolated and sharpened by the following recurrence equations.

$$R_{rec}^{(n+1)} = L_r \left[R_{rec}^{(n)} + \varepsilon \cdot A^* \bullet (R_{obs} - A \bullet R_{rec}^{(n)}) \right] \tag{8}$$

, L_r : frequency-band limitation for the red plane

$$B_{rec}^{(n+1)} = L_b \left[B_{rec}^{(n)} + \varepsilon \cdot A^* \bullet (B_{obs} - A \bullet B_{rec}^{(n)}) \right] \tag{9}$$

, L_b : frequency-band limitation for the blue plane

where the operators L_r, L_b limit the frequency components of the updated images $R_{rec}^{(n)}$, $B_{rec}^{(n)}$ within their fundamental frequency pass-bands. In these cases, the fundamental frequency pass-bands corresponding to the sub-sampling patterns of the mosaicked red and blue pixels are different from that of the mosaicked green ones. Figure 1(b) illustrates these frequency-band limitations.

3.2. Problem of the sharpening-demosaicking approach

The human visual system is much more sensitive to high frequency components of the luminance than to those of the chrominance. The idea of the Bayer's color filter array takes advantage of this property. For most images, this property holds true, but it sometimes loses its validity for images that contain very sharp color edges. This invalidation has its root in the fact that the pass-band of the demosaicked green image is different from those of the demosaicked red and blue images when the sharpening-demosaicking method is applied to images mosaicked with the Bayer's color filter array.

4. USE OF THE WRB COLOR FILTER ARRAY

For the sharpening-demosaicking approach, it is desirable that RGB colors should be equally mosaicked on the 2-D imaging surface, and hence the mosaicking pattern with the equilateral triangular lattice is preferable. However, the triangular mosaicking is not popular. Instead of the optimal triangular mosaicking, this paper employs another suboptimal approach: the other combination of color filters where the green filters in the Bayer's RGB color filter array are replaced by the white (W) filters. The white filtering means that all the visible light passes through it. Therefore, intensity of the pixel filtered by the white filter, called the white pixel intensity for short, will be almost equal to the sum of its corresponding red, green and blue intensity values, and the white pixel intensity conveys information over the wide spectrum-band of the incident light. Such information may be utilized for demosaicking and sharpening RGB color intensity values. The problem is how to separate RGB color intensity values from the observed white pixel intensity value. To solve the problem, this paper extends the Landweber-type sharpening-demosaicking algorithm for the Bayer's RGB filter array.

The sharpening-demosaicking algorithm updates the value of each demosaicked color pixel from the observed mosaicked color pixels whose values are given by integrating color intensity within the adjacent portion of the size of vertically and horizontally

twice the pixel interval. In the case of the WRB filter array, the image portion for the spatial integration of the white pixel and that of its adjacent red or blue pixel partially overlap each other. Hence, the similar Landweber-type sharpening-demosaicking algorithm can restore spatially integrated pixels and can separate red, green and blue intensity values from the observed white intensity value.

In the case of the WRB filter array, unlike the RGB filter case, the Landweber-type recursion equations for the three color components are linked each other. The coupled recursion formulae are given by equation (10) where W_{obs}, R_{obs} and B_{obs} mean the observed mosaicked white, red and blue images, respectively; whereas R_{rec}, G_{rec} and B_{rec} denote iteratively updated demosaicked red, green and blue images, respectively. The coupled update of equation (10) is followed by the application of the frequency-band limitation L_w, corresponding to the sub-sampling pattern of the white pixels in the WRB color filter array, to each updated primary color image, as shown by equation (11). The operator L_w is identical with the operator L_g mentioned above.

5. PERFORMANCE EVALUATIONS

For performance evaluations, we take into account the three factors: the color reproduction, the restoration of high spatial-frequency components and the robustness to shot noise.

5.1. Color reproduction

We use the Macbeth color chart to evaluate the color response. We make the WRB-mosaicked Macbeth color chart image through computer simulation. First, we produce the sufficiently high-resolution multi-spectrum images based on the spectral reflectance of the Macbeth color chart, and then we simulate the optical low-pass filtering by integrating intensity values within the image portion of the size of vertically and horizontally twice the pixel interval in each multi-spectrum image. Next, we transform these multi-spectrum images into the WRB images by integrating the multi-spectrum images multiplied by both the spectral transmittance of the WRB color filters and the spectral sensitivity of the solid-state imaging device. Finally, each of the full-resolution WRB images is sub-sampled according to the mosaicking pattern of its corresponding color filter.

We use this WRB-mosaicked image, and reconstruct RGB color components from it with our sharpening-demosaicking method. To evaluate its color reproduction, we define the reference RGB color image as follows: we produce the non-mosaicked RGB color image by taking into account the above-mentioned factors and the spectral transmittance of the red, green and blue color filters, and we use it as the reference RGB color image. Figure 2(a) shows the reference RGB color image and figure 2(b) shows the restored RGB color image given by our sharpening-demosaicking method. This result shows that our proposed sharpening-demosaicking method can restore the RGB color components from the WRB-mosaicked image accurately.

$$
\begin{cases}
G_{rec}^{(n+1)} = G_{rec}^{(n)} + \varepsilon \cdot A * \bullet G^{(n)} \\
\quad ,[G^{(n)}]_{(i,j)} = \begin{cases} [W_{obs} - A \bullet ((R_{rec}^{(n)} + G_{rec}^{(n)} + B_{rec}^{(n)})/3)]_{(i,j)} & ;\ if\ (i,j)\ is\ a\ site\ of\ an\ observed\ white\ pixel \\ 0 & ;\ if\ (i,j)\ is\ a\ site\ of\ an\ observed\ red\ or\ blue\ pixel \end{cases} \\
R_{rec}^{(n+1)} = R_{rec}^{(n)} + \varepsilon \cdot A * \bullet R^{(n)} \\
\quad ,[R^{(n)}]_{(i,j)} = \begin{cases} [W_{obs} - A \bullet ((R_{rec}^{(n)} + G_{rec}^{(n)} + B_{rec}^{(n)})/3)]_{(i,j)} & ;\ if\ (i,j)\ is\ a\ site\ of\ an\ observed\ white\ pixel \\ [R_{obs} - A \bullet R_{rec}^{(n)}]_{(i,j)} & ;\ if\ (i,j)\ is\ a\ site\ of\ an\ observed\ red\ pixel \\ 0 & ;\ if\ (i,j)\ is\ a\ site\ of\ an\ observed\ blue\ pixel \end{cases} \\
B_{rec}^{(n+1)} = B_{rec}^{(n)} + \varepsilon \cdot A * \bullet B^{(n)} \\
\quad ,[B^{(n)}]_{(i,j)} = \begin{cases} [W_{obs} - A \bullet ((R_{rec}^{(n)} + G_{rec}^{(n)} + B_{rec}^{(n)})/3)]_{(i,j)} & ;\ if\ (i,j)\ is\ a\ site\ of\ an\ observed\ white\ pixel \\ [B_{obs} - A \bullet B_{rec}^{(n)}]_{(i,j)} & ;\ if\ (i,j)\ is\ a\ site\ of\ an\ observed\ blue\ pixel \\ 0 & ;\ if\ (i,j)\ is\ a\ site\ of\ an\ observed\ red\ pixel \end{cases}
\end{cases}
\tag{10}
$$

$$
G_{rec}^{(n+1)} \leftarrow L_w[G_{rec}^{(n+1)}] \quad ; \quad R_{rec}^{(n+1)} \leftarrow L_w[R_{rec}^{(n+1)}] \quad ; \quad B_{rec}^{(n+1)} \leftarrow L_w[B_{rec}^{(n+1)}] \tag{11}
$$

5.2. Restoration of high spatial-frequency components

We use the artificially generated windmill chart to evaluate the ability of restoring high spatial-frequency components. We generate the WRB-mosaicked image of the color windmill chart through computer simulation. We produce the image in the same manner as described in 5.1. We restore the RGB color image from the WRB-mosaicked image. Figure 3(a) shows the image restored by our sharpening-demosaicking method from the WRB-mosaicked image, and figure 3(b) shows the image restored by the ACPI [3] from the RGB-mosaicked image. In figure 3(b), the ACPI produces undesirable artifacts even for low-frequency image portions in the diagonal directions, whereas our sharpening-demosaicking method does not produce such artifacts. Our sharpening-demosaicking method restores high frequency components better than the ACPI , but as side effects it somewhat amplifies aliasing artifacts at the image portions of high frequencies close to the Nyquist frequencies.

5.3. Robustness to shot noise

We model the additive shot noise of the photoelectric conversion as signal-dependent Gaussian noise whose variance depends on signal power. We add Gaussian noise to the WRB-mosaicked Macbeth color chart image, and restore the RGB color image by

(a) Reference RGB color image (b) Restored image by our sharpening-demosaicking method

Figure 2: Evaluation of the color reproduction.

our sharpening-demosaicking method, and then calculate the peak SNR of each of the restored RGB color components to the non-mosaicked noise-free ones. Figure 4 shows the evaluation results. For comparison, we show the peak SNR of the demosaicked red and green components recovered from the RGB-mosaicked noise-added image by the constant hue base method [1] and the ACPI [3]. Our sharpening-demosaicking method uses the wide spectrum-band white pixel intensity instead of the green pixel intensity, and hence a lager amount of shot noise added to the white pixels spreads over the three primary color components. Our sharpening-demosaicking method has a tendency to amplify shot noise, and hence the robustness of our sharpening-demosaicking method to shot noise is weaker than that of the existing demosaicking methods using RGB filter array.

5.4. Evaluation using a natural image

Figure 5 compares an enlarged part of the demosaicked color image recovered by our sharpening-demosaicking method from the artificially generated WRB-mosaicked image, with that recovered by the ACPI using the RGB filter array from the artificially generated RGB-mosaicked image. Our sharpening-demosaicking method provides a slightly sharper image than the ACPI. Sharpness improvements are visible particularly in the image regions of hairlines and eyes.

6. CONCLUSIONS

In the ability of restoring high spatial-frequency components our sharpening-demosaicking method using the WRB color filter array is superior to the existing demosaicking methods using the RGB color filter array. However, in the robustness to shot noise, our sharpening-demosaicking method is inferior to the existing demosaicking methods.

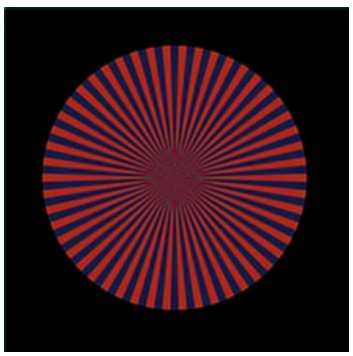

(a) Our sharpening-demosaicking method using the WRB color filter array

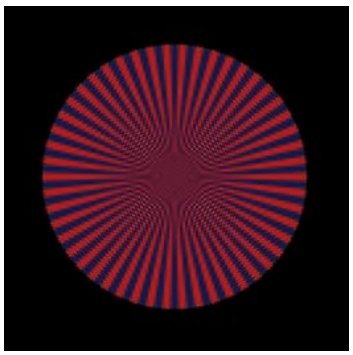

(b) ACPI demosaicking method using the RGB color filter array

Figure 3: Comparison of the ability of restoring high spatial-frequency components.

7. REFERENCES

[1] D. R. Cok : Signal processing method and apparatus for producing interpolated chrominance values in a sampled color image signal, United States Patent 4,642,678, 1987.

[2] C.A. Laroche and M.A. Prescott : Apparatus and method for adaptively interpolating a full color image utilizing chrominance gradients, United States Patent 5,373,322, 1994.

[3] J.F. Hamilton Jr. and J.E. Adams : Adaptive color plan interpolation in signal sensor color electronic camera, United State Patent, 5,629,734, 1997.

[4] F. Malgouyres and F. Guichard : Edge direction preserving image zooming: a mathematical and numerical analysis, *SIAM J. Num. Anal.*, **39**, pp.1-37, 2001.

[5] L. Landweber : An iteration formula for Fredholm integral equations of the first kind, *Am. J. Math.*, **73**, pp.615-624, 1951.

[6] S.P. Kim and N.K. Bose : Reconstruction of 2-D band-limited discrete signals for non-uniform samples, *Proc. IEE-F*, **137**, pp.197-204, 1990.

[7] H.J. Trussel and R.E. Hartwing : Mathematics for Demosaicking, *IEEE Trans. Image Processing,* **11**, 4, pp.485-492, April 2002.

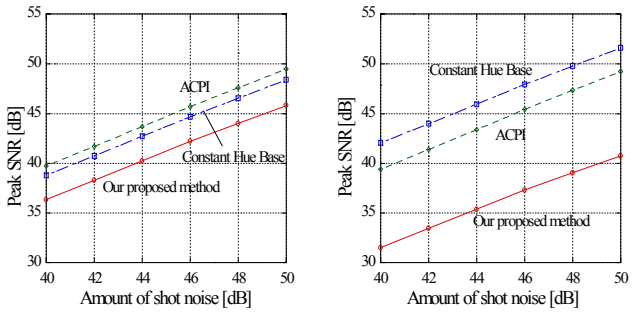

(a) Red image (b) Green image

Figure 4: Evaluation of the robustness to shot noise.

(a) Our sharpening-demosaicking method using the WRB color filter array

(b) ACPI demosaicking method using the RGB color filter array

Figure 5: Enlarged parts of the demosaicked color images.